Extended-range propagated order in amorphous solids

1994 J. Phys.: Condens. Matter 6 L99

(http://iopscience.iop.org/0953-8984/6/8/001)

J. Phys.: Condens. Matter 6 (1994) L99–L105. Printed in the UK

LETTER TO THE EDITOR

Extended-range propagated order in amorphous solids

A Uhlherr† and S R Elliott

Department of Chemistry, University of Cambridge, Lensfield Road, Cambridge CB2 1EW, UK

Received 20 December 1993

Abstract. Atomic density fluctuations, extending to at least 35 Å, have been discovered in a large (13 824 atom) model of amorphous silicon (a-Si). This extended-range structural order has been found, in the case of a-Si, to arise from second-neighbour correlations preferentially propagating atomic-density fluctuations. The period of such low-amplitude, extended-range oscillations in atomic density, namely $\simeq$3.4 Å in the case of a-Si, is that associated with the position of the first sharp diffraction peak (FSDP), namely $\simeq$1.9 Å^{-1}; indeed, the extended real-space fluctuations for $r > 10$ Å contribute almost as significantly to the intensity of the FSDP as do the much stronger, but less periodic, correlations in the range 0–10 Å.

The structure of non-crystalline covalent networks (amorphous solids, glasses and liquids) is widely believed to consist of an appreciable degree of chemical short-range order over lengths <5 Å, possibly some medium-range order (5–20 Å), but no order at longer ranges [1]. While medium-range order is manifested experimentally by structural features such as the first sharp diffraction peak [2] and the Raman 'boson' peak [3], their interpretation has remained controversial [4]. Structural models and simulations have contributed a great deal to our understanding of such materials [5, 6], but have generally been restricted to length scales ~10 Å. In this letter we use results from large models of amorphous silicon [7, 8] to show that interatomic correlations can be discerned over rather greater distances (>30 Å, possibly ~60 Å) than previously supposed, and that these extended-range correlations are directly responsible for the first sharp diffraction peak. The structure of amorphous network materials is generally characterized by the pair distribution function $g(r)$, which represents the atomic number density at a distance r from an origin atom, normalized by the bulk number density ρ_0. Fourier transformation yields the structure factor $S(Q)$, where a point Q in reciprocal space corresponds to an oscillation of period R in real space as given by the simple relationship $QR = 2\pi$ [9]. The experimental structure factor of amorphous silicon (a-Si), as measured by neutron diffraction [10], contains a first sharp diffraction peak (FSDP) at $Q \simeq 1.9$ Å^{-1}. Figure 1 shows the pair distribution function $g(r)$, resulting from the Fourier transformation of *only* the FSDP portion of Fortner and Lannin's structure factor for annealed a-Si [10]. The mean period R of oscillation in $g(r)$ is $\simeq$3.3 Å, as expected, when measured over the entire range of $\simeq$55 Å. Over shorter ranges the period is significantly greater—for example the first peak occurs at 3.9 Å—confirming that the widely-adopted assumption of Debye–Scherrer behaviour for the FSDP [1, 11] (real-space atomic

† Present address: CSIRO Division of Chemicals and Polymers, Private Bag 10, Clayton, 3168 Australia.

0953-8984/94/080099+07$19.50

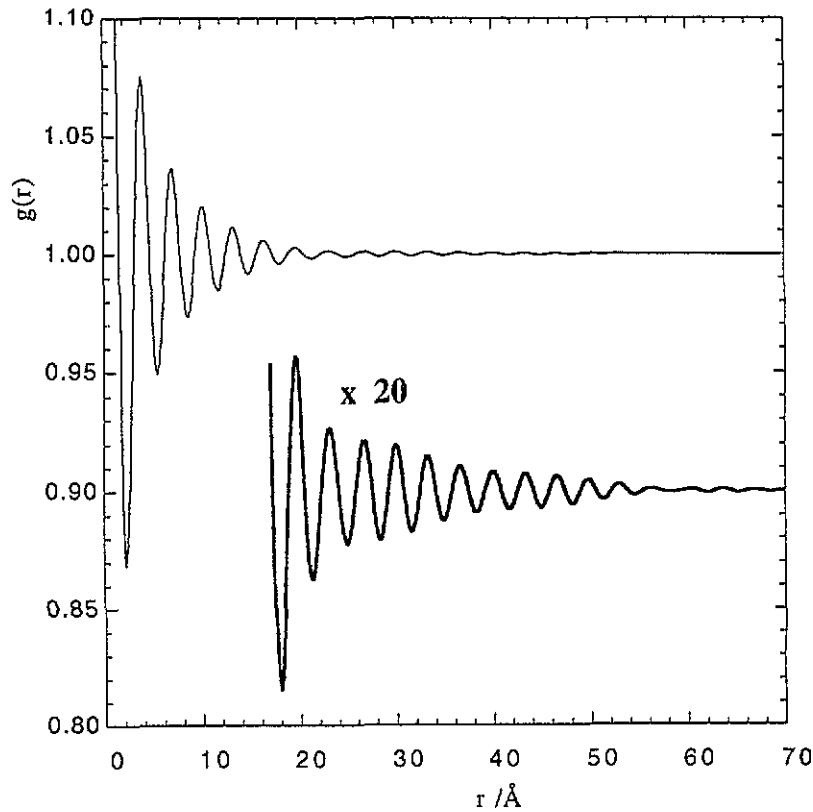

Figure 1. Pair distribution function $g(r)$ corresponding to Fourier transformation of the first peak in the experimental structure factor, $S(Q)$, of amorphous silicon. The neutron diffraction data of Fortner and Lannin [10] for annealed a-Si was smoothed using a cubic spline with a point spacing of 0.001 Å^{-1} to enhance the resolution artificially, then truncated below 1.840 Å^{-1} and above 2.224 Å^{-1}, the two Q points where $S(Q) = 1$. The inset shows an enlargement of the $g(r)$ curve for large r, which has been displaced vertically for clarity.

density fluctuations of uniform period, decaying exponentially to vanish within $\simeq$20 Å) is misleading.

Figure 2(a) shows the pair distribution function of a 13824 atom model of a-Si generated by Holender and Morgan [8]. For $r > 10$ Å the model $g(r)$ shows qualitatively similar behaviour to the experimentally-derived data in figure 1, with a mean period of oscillation $R \simeq 3.4$ Å over the full range 0–33 Å defined by the size of the model. The weak, extended real-space fluctuations for $r > 10$ Å contribute almost as significantly to the intensity of the model FSDP [8] as do the much stronger but *less periodic* correlations in the range 0–10 Å. We note in passing that the pair distribution function of Holender and Morgan's largest, 110592 atom structure [8] shows well-resolved oscillations in $g(r)$ extending to 66 Å, but the amplitude of the oscillations >33 Å is enhanced by a period doubling artefact resulting from the annealing procedure; we will thus not consider this structure further.

$g(r)$ can be resolved into separate contributions $g_n(r)$ due to nth neighbours of the origin atom, where n denotes the *shortest* bond percolation path between the two atoms [12]. By definition, the first peak in $g(r)$ is entirely due to nearest neighbours, while the second peak is dominated, unsurprisingly, by second-neighbour atoms. The third neighbour-specific pair distribution, $g_3(r)$, is a broad double peak, reflecting a non-uniform distribution of dihedral

angles [4]. The form of the doublet can be related to the ring statistics of the model, as shown in figure 2(*b*).

Intriguingly, $g_4(r)$ is a single peak which is considerably narrower than $g_3(r)$, a result of the strong inverse correlation between pairs of successive dihedral angles (n = 0–3, 1–4). Such directional constraints evidently also occur for more distant neighbours. Table 1 shows that the $g_n(r)$ form a well-defined and almost evenly spaced sequence of approximately Gaussian distributions for n = 5–13, with very slowly varying widths and intensities. Over the intermediate range n = 3–10, the even-n peaks are clearly narrower and more intense than the odd-n peaks. The separation between neighbouring (odd–even) peaks is $\simeq$1.7 Å; the separation of *alternate* (even–even or odd–odd) peaks is thus $\simeq$3.4 Å. While the positions of the maxima and minima in $g(r)$ do *not* appear to coincide with the $g_n(r)$ peaks, the fluctuations in $g(r)$ are clearly a consequence of the radial symmetry of successive neighbour shells as characterized by the $g_n(r)$. The inset to figure 2(*a*) suggests that one might expect such symmetry to extend beyond n = 13, the numerical limit of our quantitative neighbour analysis.

Table 1. Characteristics of the neighbour-specific pair distribution functions $g_n(r)$ for the 13824-atom room-temperature model of a-Si [8]. FWHM is the full width at half maximum of $g_n(r)$, while r_n is the observed peak position, c_n is the total number of nth neighbours per atom, defined as $c_n = 4\pi\rho_0 \int_0^\infty r^2 g_n(r)\,dr$ where ρ_0 is the bulk density. The ratio $c_n/(c_{n-1}c_1)$ thus represents the number of nth neighbours as a fraction of the number of atoms bonded to each $(n-1)$th neighbour. I_n^*, r_n^*, σ^* and R denote intensity, peak position, width (standard deviation) and correlation coefficient, respectively, for non-linear least-squares fits of Gaussian distributions to $g_n(r)$.

n	FWHM/Å	r_n/Å	c_n	$c_n/(c_{n-1}c_1)$	I_n^*	r_n^*/Å	σ^*/Å	R
1	0.19	2.38	4.02	1.000	5.770(23)	2.385(1)	0.078(1)	0.9964
2	0.60	3.83	12.07	0.747	1.960(6)	3.831(1)	0.271(1)	0.9982
3	1.91	5.74	26.84	0.553	0.717(2)	4.667(3)	0.472(1)	0.9996
					0.871(2)	5.763(2)	0.362(1)	
4	1.63	6.96	47.96	0.445	0.936(2)	6.961(2)	0.707(2)	0.9984
5	2.06	8.67	76.28	0.396	0.845(2)	8.601(2)	0.830(2)	0.9990
6	1.91	10.27	111.2	0.362	0.851(1)	10.346(1)	0.820(1)	0.9999
7	2.11	12.12	153.4	0.343	0.809(1)	12.085(1)	0.877(1)	0.9998
8	2.10	13.80	202.7	0.329	0.799(1)	13.851(1)	0.889(1)	0.9998
9	2.25	15.69	259.3	0.318	0.771(1)	15.629(1)	0.928(1)	0.9998
10	2.24	17.46	323.2	0.310	0.760(1)	17.412(1)	0.945(1)	0.9997
11	2.31	19.19	394.6	0.304	0.740(1)	19.212(1)	0.973(1)	0.9998
12	2.36	20.97	473.5	0.299	0.728(1)	21.008(1)	0.993(1)	0.9997
13	2.39	22.78	559.8	0.294	0.715(1)	22.821(1)	1.012(1)	0.9998

The source of the extended-range radial density fluctuations for $r > 10$ Å is considered in figure 3. The location of an nth neighbour atom, i, at a specified distance r_i from the origin, influences $g(r)$ for $r > r_i$, because some of the (Δn)th neighbours of i are $(n + \Delta n)$th neighbours of the origin atom, with a shortest path that includes i. Figure 3 shows that Δn = 1 correlations reflect a rather broad range of *radial* separations between nearest neighbours, because of the variation of possible orientations of individual bonds which is imposed by tetrahedral coordination. The abundance of 6- and 7-membered rings, and the concomitant variability in the dihedral angle, results in a wide range of Δn = 3 separations, while the range of separations for $\Delta n > 3$ increases due to an accumulation of the inherent variation in lengths of individual bonds. Hence, the significant contribution to the radial atomic density by neighbours of i is due to Δn = 2 correlations, and occurs at r_i + 3.4 Å. Thus we may predict that an existing feature of $g(r)$ at r_i (i.e. a peak or trough)

(*a*)

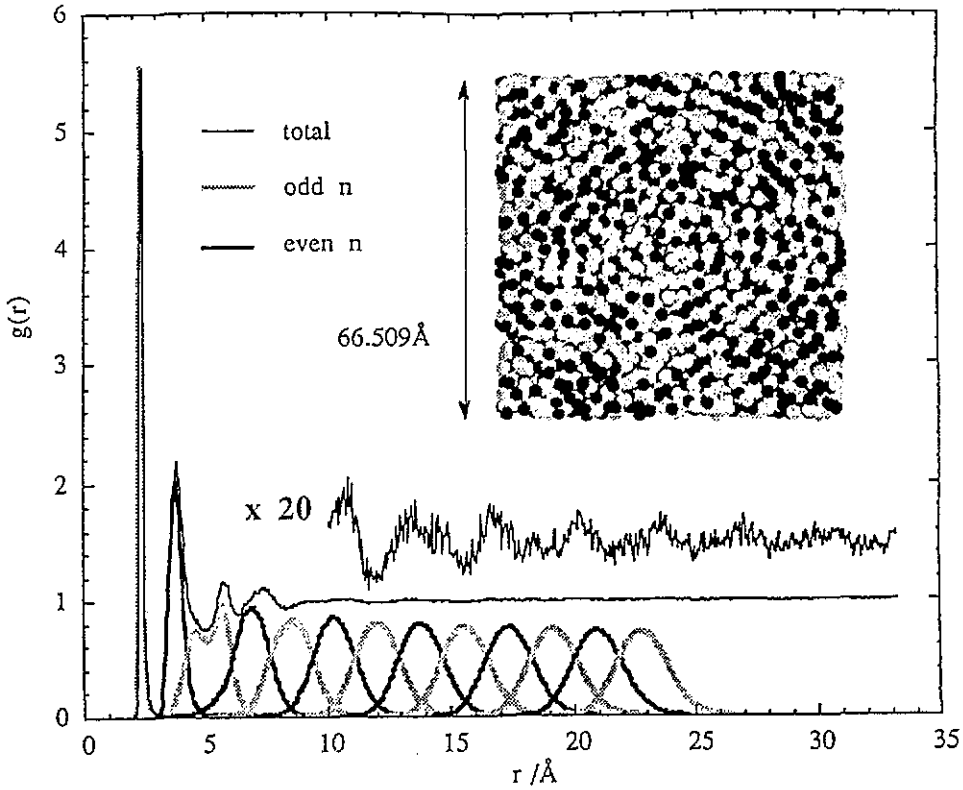

Figure 2. Pair distribution function $g(r)$ of a 13824-atom room-temperature model of a-Si [8], resolved into contributions $g_n(r)$ due to nth neighbour atoms. Each atom is classified as an nth neighbour, where n is the *minimum* number of bonds between it and the origin atom (note that all pairs of atoms which contribute to the first peak in $g(r)$, i.e. all pairs separated by less than 3.0 Å, are defined as being bonded). For a given origin, each atom thus has a unique value of n, hence $g(r) = \sum_n g_n(r)$; $g_n(r)$ and $g(r)$ are then averaged over all origin atoms. (*a*) Total $g(r)$ and $g_n(r)$, n = 1–13. The inset shows a projected top view of a 12 Å thick 'slice' through the model. The section contains 2476 atoms, including an origin atom at the centre. Odd neighbours ($n = 1 \rightarrow 25$) of the origin atom are drawn in grey, even neighbours $n = 2 \rightarrow 26$) are black. Relative to the scale of the projection, the Si atoms are depicted as being somewhat smaller than their true covalent radii. (*b*) $g_n(r)$, n = 3–4. $g_3(r)$ is resolved into contributions due to third neighbours located in m-membered rings, m = 6–11, using the shortest path (SP) ring formalism [26]. Note that five-membered rings are also quite abundant—24% of all SP rings in this model—but by definition do not contain any third neighbours. An 'open' path corresponds to the case where the origin and third neighbour atoms do not share a common SP ring. The inset depicts a simple example of a configuration where the origins A and D generate the same fourth neighbour distance, AD, via two different third neighbour distances, BD and AC (AC').

will be *propagated* with a period $\simeq$3.4 Å, irrespective of the exact positions of the $g_n(r)$ peaks.

The first peak in the structure factor of a-Si at Q = 1.9 Å^{-1} [10] is thus associated with extended-range atomic density fluctuations, of approximately radial symmetry about *each* atom, as seen in figure 2(*a*). Similar conclusions have been drawn previously by Cervinka *et al* [13] for abstract two-dimensional networks. We have described the source of these atomic density fluctuations in terms of angular constraints; an equally valid, complementary depiction is of a chemical-ordered packing of atoms and interatomic 'voids' [14–16], a topic

(*b*)

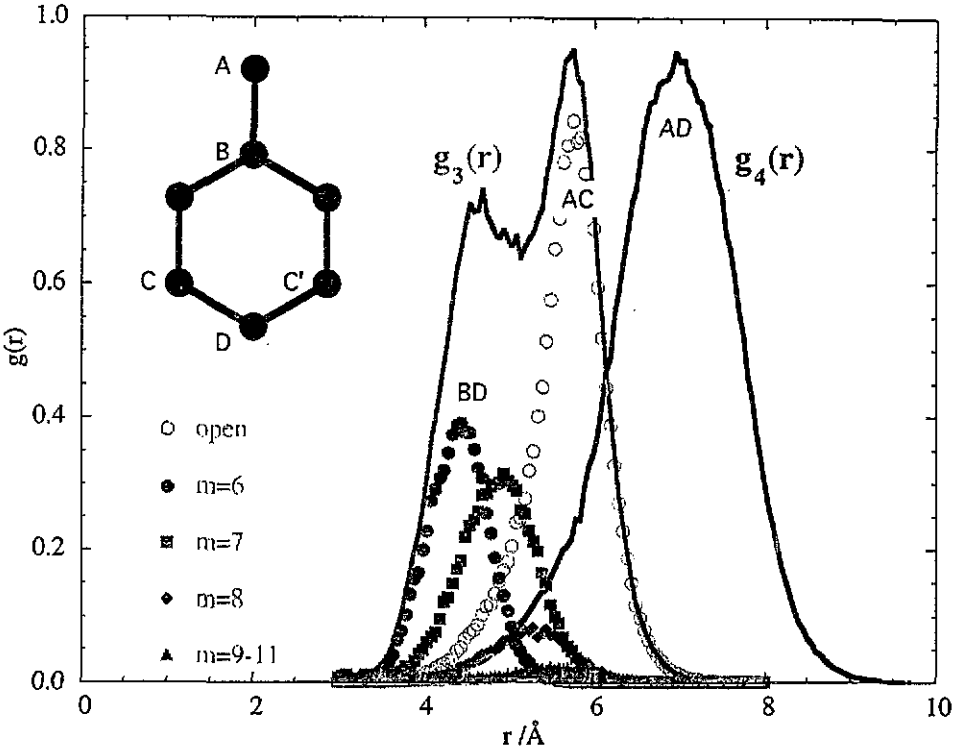

Figure 2. *continued.*

which will be discussed fully in a future publication.

A first sharp diffraction peak (FSDP) is also observed in the more archetypal oxide/chalcogenide glasses and melts [2, 4]. For example, the structure of silica glass can be well approximated by 'decorating' a-Si with oxygen atoms [17]; from the ratio of Si–Si separations for the two materials, one may correctly predict the existence of an FSDP for SiO_2 at Q = 1.5 $Å^{-1}$ [18]. Similar scaling approximations may be applied to the FSDPs of other AX_2 glasses such as $GeSe_2$ or BeF_2 [2]. By analogy with a-Si, one would thus expect the FSDP of AX_2 systems to be due to $\Delta n = 4$ correlations (A–X–A–X–A, X–A–X–A–X). We have found that this is true of the FSDP in Feuston and Garofalini's model of SiO_2 glass [19], although the small size (648) atoms obviously reduces the contribution of extended-range correlations to the FSDP, and hence limits the scope for agreement between calculated and experimental $S(Q)$. Interestingly, early x-ray diffraction measurements on silica glass revealed fine structure in $g(r)$ to at least 20 Å, which at the time was attributed to tridymite-like microcrystallinity [20].

It thus seems likely that extended low-amplitude periodicity in $g(r)$ is a structural characteristic common to many amorphous materials. In a single-component tetrahedral network such as a-Si, the extended-range structure results from $\Delta n = 2$ correlations, which are defined by the short-range order, $n \leqslant 2$. In multicomponent systems it is the medium-range order which is propagated (e.g. $\Delta n = 4$ in SiO_2 and related glasses). While this letter has concentrated on affirming the presence of extended-range structure in tetrahedral networks of high connectivity, its existence is also anticipated in amorphous solids with

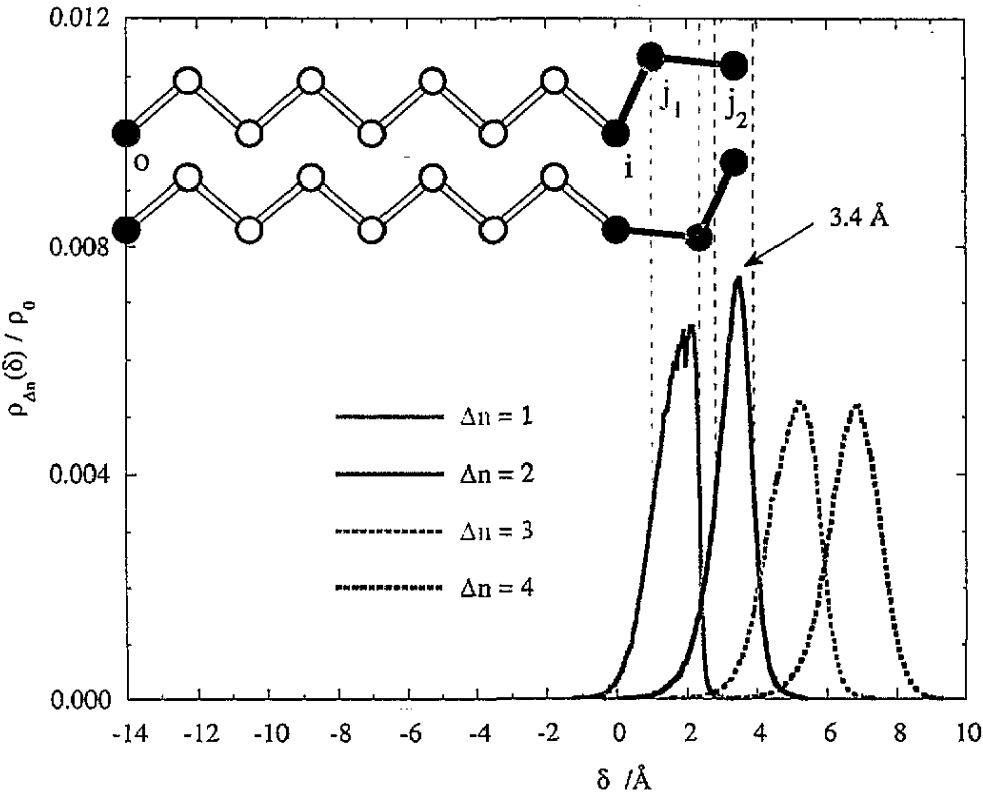

Figure 3. Density distribution of atoms j in the vicinity of an atom i located a fixed distance r_i from an origin atom O, as a function of $\delta = r_j - r_i$, namely the difference in the distances of i and j from the origin. $\rho_{\Delta n}(\delta)$ is represented as the number density per atom i, while ρ_0 denotes the bulk number density. In this example, atoms i are chosen so that $r_i = 14.00 \pm 0.05$ Å. Labelling i as an nth neighbour of O, *where n is variable* (in this case approximately 7% n = 7, 78% n = 8 and 15% n = 9, see figure 2(*b*)), distributions are shown for those j which are $(n + \Delta n)$th neighbours of O, Δn = 1–4. The atoms j are thus respective subsets of the first, second, third and fourth neighbours of i. The curves were evaluated over all origin atoms O for Holender and Morgan's 13824-atom room-temperature model of a-Si [8]. The dashed vertical lines represent the widths (FWHM) of the distributions $\rho_{\Delta n}(\delta)$, Δn = 1, 2. The variation of $\rho_{\Delta n}(\delta)$ with r_i (>10 Å) is weak, but complex (Uhlherr and Elliott, in preparation). The inset schematic is an illustrative example of how the tetrahedral symmetry about each atom (in this case j_1), combined with the fact that shortest percolation paths become roughly linear with increasing n, imposes a greater directional constraint (and hence greater constraint on δ) for Δn = 2 pairs $(i - j_2)$ than for Δn = 1 pairs $(i - j_1)$.

chain-like ($SiSe_2$, AgI-$AgPO_3$) or sheet-like (B_2O_3) structures, and indeed in liquids with FSDPs such as As_2Se_3 or $GeSe_2$ [21, 22]. In such materials, extended-range order is thus envisaged to originate not from pseudocrystalline fragments [23], randomly packed clusters [24] or layers [25], but simply from the topology of the random network.

The authors are very grateful to J M Holender and G J Morgan, for providing coordinates of a-Si models, and also to S H Garofalini, for supplying a-SiO_2 model coordinates. It is a pleasure to acknowledge the financial assistance of the EC and the Isaac Newton Trust of Trinity College, Cambridge.

References

[1] Elliott S R 1990 *Physics of Amorphous Materials* 2nd edn (London: Longman) pp 73–169
[2] Moss S C and Price D L 1985 *Physics of Disordered Materials* ed D Adler, H Fritzsche and S R Ovshinsky (New York: Plenum) pp 77–95
[3] Novikov V N and Sokolov A P 1991 *Solid State Commun.* **77** 243–7
[4] Elliott S R 1991 *Nature* **354** 445–52
[5] Wright A C, Hulme R A, Grimley D I, Sinclair R N, Martin S W, Price D L and Galeener F L 1990 *J. Non-Cryst. Solids* **129** 213–32
[6] Soules T F 1990 *J. Non-Cryst. Solids* **123** 48–70
[7] Holender J M and Morgan G J 1991 *J. Phys.: Condens. Matter* **3** 1947–52
[8] Holender J M and Morgan G J 1991 *J. Phys.: Condens. Matter* **3** 7241–54
[9] Hansen J-P and McDonald I R 1990 *Theory of Simple Liquids* 2nd edn (London: Academic) pp 97–104
[10] Fortner J and Lannin J S 1989 *Phys. Rev.* B **39** 5527–30
[11] Sokolov A P, Kisliuk A, Soltwisch M and Quitmann D 1992 *Phys. Rev. Lett.* **69** 1540–3
[12] Temkin R J 1978 *J. Non-Cryst. Solids* **28** 23–44
[13] Cervinka L, Komrska J and Mikes J 1985 *J. Non-Cryst. Solids* **75** 69–74
[14] Bletry J 1990 *Phil. Mag.* B **62** 469–508
[15] Elliott S R 1991 *Phys. Rev. Lett.* **67** 711–4
[16] Elliott S R 1992 *J. Phys.: Condens. Matter* **4** 7661–78
[17] Wright A C, Connell G A N and Allen J W 1980 *J. Non-Cryst. Solids* **42** 69–86
[18] Susman S, Volin K J, Liebermann R C, Gwanmesia G D and Wang Y 1991 *Phys. Chem. Glasses* **31** 144–50
[19] Feuston B P and Garofalini S H 1988 *J. Chem. Phys.* **89** 5818–24
[20] Konnert J H, Karle J and Ferguson G A 1973 *Science* **179** 177–9
[21] Uemura O, Sagara Y, Muno D and Satow T 1978 *J. Non-Cryst. Solids* **30** 155–62
[22] Penfold I T and Salmon P S 1991 *Phys. Rev. Lett.* **67** 97–100
[23] Cervinka L 1988 *J. Non-Cryst. Solids* **106** 291–300
[24] Price D L, Moss S C, Reijers R, Saboungi M L and Susman S 1988 *J. Phys. C: Solid State Phys.* **21** L1069–72
[25] Busse L E 1984 *Phys. Rev.* B **29** 3639–51
[26] Franzblau D S 1991 *Phys. Rev.* B **44** 4925–30